



Deposited via The University of Leeds.

White Rose Research Online URL for this paper:

<https://eprints.whiterose.ac.uk/id/eprint/98770/>

Version: Accepted Version

---

**Article:**

Khaemba, DN, Neville, A and Morina, A (2016) New insights on the decomposition mechanism of Molybdenum Dialkyl-diThioCarbamate (MoDTC): a Raman spectroscopic study. RSC Advances, 6 (45). pp. 38637-38646. ISSN: 2046-2069

<https://doi.org/10.1039/C6RA00652C>

---

**Reuse**

Items deposited in White Rose Research Online are protected by copyright, with all rights reserved unless indicated otherwise. They may be downloaded and/or printed for private study, or other acts as permitted by national copyright laws. The publisher or other rights holders may allow further reproduction and re-use of the full text version. This is indicated by the licence information on the White Rose Research Online record for the item.

**Takedown**

If you consider content in White Rose Research Online to be in breach of UK law, please notify us by emailing [eprints@whiterose.ac.uk](mailto:eprints@whiterose.ac.uk) including the URL of the record and the reason for the withdrawal request.

# **New insights on the decomposition mechanism of Molybdenum DialkyldiThioCarbamate (MoDTC): A Raman spectroscopic study**

Doris N Khaemba\*, Anne Neville, Ardian Morina

Institute of Functional Surfaces, School of Mechanical Engineering, University of Leeds, LS2 9JT Leeds, United Kingdom (UK).

\*Corresponding author. Email: d.n.khaemba@leeds.ac.uk

## **Abstract**

Molybdenum DialkyldiThioCarbamate (MoDTC) is a friction modifier that has been used in automotive engines for many years. However, its exact decomposition mechanism within tribocontacts is not fully understood. In this study, an attempt has been made towards understanding the mechanism of MoDTC decomposition in steel/steel contacts by employing Raman spectroscopy. Results show that the main MoDTC decomposition products are MoS<sub>2</sub>, FeMoO<sub>4</sub> and sulphur-rich molybdenum compounds, MoS<sub>x</sub> (x>2), in contrast to the previously reported MoS<sub>2</sub> and MoO<sub>3</sub>. Formation of these products is dependent on tribological parameters. Raman results from this study indicate that the Mo<sup>6+</sup> species previously observed in X-ray Photoelectron Spectroscopy (XPS) analysis are probably from FeMoO<sub>4</sub> and not MoO<sub>3</sub>. This paper presents an alternative reaction pathway for MoDTC decomposition in steel/steel contacts with MoS<sub>x</sub> as an intermediate product and MoS<sub>2</sub> as the final product. FeMoO<sub>4</sub> is formed from a side reaction of iron oxides with molybdenum compounds at low temperatures and low MoDTC concentrations. Results also show that friction is dependent on the nature of decomposition products at the tribocontact. Knowledge of MoDTC decomposition reaction pathway will enable the friction performance of MoDTC lubricants to be optimized.

## 1 Introduction

Lubricants play an important role in different engineering systems. In the automotive industry, engine lubricants are key to ensuring the effective performance of internal combustion engines and improving fuel economy as a result. The efficiency of engine lubricants is determined by additives present in the lubricant. Of these additives, friction modifiers and antiwear additives are of particular importance especially for components operating in the boundary lubrication regime. Boundary lubrication refers to the regime where there is no substantial fluid film separating the surfaces. Friction modifiers and antiwear additives perform their various functions by decomposing at the rubbing interface (tribocontact) to form thin films commonly known as tribofilms. A good understanding of additive decomposition in tribological contacts is thus crucial in lubricant development and formulation. Although there are numerous studies on friction and wear performance of various engine lubricant additives, there are still limited studies on additive decomposition pathways and reaction kinetics.

Molybdenum DialkylthioCarbamate (MoDTC) has been used as a friction modifier in engine lubricants since early 1970s.<sup>1-3</sup> The friction performance of MoDTC-containing lubricants in steel/steel sliding contacts has been shown to be dependent on contact parameters such as temperature, additive concentration, stroke length, sliding speed and surface roughness.<sup>3-7</sup> Low friction ( $\mu=0.04-0.06$ ) has been observed when tribofilms composed of  $\text{MoS}_2$ , formed from MoDTC decomposition, are present at the tribocontact while high friction ( $\mu=0.1$ ) has been observed when only iron oxides are formed at the tribocontact.<sup>4</sup> Intermediate friction values ( $\mu=0.06-0.09$ ) have also been observed in certain test conditions. Friction behaviour of MoDTC is intimately related to the chemical species present in the tribocontact, thus, it is important to have a good understanding of the degradation process. It is appreciated that reactions involved in the degradation of MoDTC in tribocontacts cannot simply be considered by simulating the necessary temperature as one would do for thermally-activated

reactions. One reason for this is that under purely thermal conditions MoDTC decomposes to form MoS<sub>2</sub> at 300°C<sup>8</sup> while in tribological conditions MoS<sub>2</sub> is formed at 100°C.<sup>9</sup> This indicates that the rubbing motion in tribocontacts contributes to the kinetics and perhaps the mechanism of degradation of MoDTC.

A mechanism for MoDTC decomposition within tribocontacts has already been proposed based on results obtained from X-ray Photoelectron Spectroscopy (XPS) analysis.<sup>10</sup> According to this mechanism, MoDTC decomposes in two stages. In the first stage the thiocarbamate groups dissociate from the MoDTC molecule via the Mo-S bond leaving the Mo<sub>2</sub>S<sub>2</sub>O<sub>2</sub> core. In the second stage, the two thiocarbamate groups combine via the S-S bond forming thiuram disulphide while the Mo<sub>2</sub>S<sub>2</sub>O<sub>2</sub> core decomposes to form MoS<sub>2</sub> and MoO<sub>2</sub>. MoO<sub>2</sub> is further oxidized to form MoO<sub>3</sub>.

There are few unexplained aspects of the mechanism proposed by Grossiord *et al.*<sup>10</sup>. Firstly, although MoO<sub>2</sub> and MoO<sub>3</sub> have been suggested as decomposition products based on XPS analysis, the presence of these oxides has not been detected using other analysis techniques such as Raman spectroscopy.<sup>4,5</sup> XPS analysis is incapable of clearly distinguishing compounds with elements having the same oxidation state due to overlapping peaks. It is probable that Mo<sup>4+</sup> and Mo<sup>6+</sup> species detected by XPS are due to formation of other species besides MoO<sub>2</sub> and MoO<sub>3</sub> which have similar oxidation states. Raman spectroscopy, on the other hand, is capable of clearly distinguishing molybdenum species; even those with the same oxidation state. Raman spectroscopy thus provides more accurate characterization than XPS for this specific aspect of tribochemistry. Secondly, the mechanism does not explain what happens to MoDTC in conditions where MoS<sub>2</sub> is not formed or whether other MoDTC decomposition products are formed besides MoS<sub>2</sub>. The presence of other decomposition products would explain intermediate friction values observed at certain test conditions.

Understanding the mechanism for MoDTC decomposition within tribocontacts is necessary because; (1) it can be used to predict the friction performance of MoDTC lubricant and will thus be useful in numerical simulation studies (2) it provides guidance to lubrication engineers on lubricant formulation so as to optimize the friction performance of MoDTC (3) it provides a great starting point in the development of future additives with similar decomposition mechanism. To facilitate this, tribotests were conducted using a MoDTC lubricant at varying temperatures, MoDTC concentrations and contact pressures. MoDTC decomposition products formed on the rubbing surfaces after tests were analysed using Raman spectroscopy.

## 2 Experimental section

### 2.1 Tribological tests

Tribotests were conducted using a high speed ball-on-disc tribometer under unidirectional sliding conditions. Steel discs used had a thickness of 1 mm and an outer diameter and inner diameter of 42 mm and 25 mm, respectively. The steel ball used had a diameter of 6.5 mm. The ball was fixed while the disc rotated against the fixed ball generating a circular wear scar on the disc. Information on test materials and test conditions is shown in Table 1.

**Table 1. Tests conditions used in the tribotests**

Test condition	Parameters
Base oil	Group III mineral oil
MoDTC concentration	0.1-0.9 wt%
Temperature	20-100°C
Contact pressure	0.98 - 2.12 GPa
Sliding speed	200 rpm (0.3 m/s), 400 rpm (0.6 m/s)
Test duration	2h
Material	Disc: AISI 1050, Ball: AISI 52100
Hardness	Disc: 60-64 HRC, Ball: 60-67 HRC
Young's Modulus	190-210 GPa (Ball and disc)
Roughness	Disc: $R_a=177$ nm, Ball: $R_a= 10$ nm
Lambda ratio ( $\lambda$ )	0.02-0.13 (Boundary lubrication regime)

To study the influence of temperature, tribotests were conducted with 0.5 wt% MoDTC at 200 rpm (0.3 m/s), 2.12 GPa. Tests were conducted at room temperature (20°C), 40°C, 60°C and 100°C. To study the influence of MoDTC concentration, tribotests were conducted at 400 rpm (0.6 m/s), 1.67 GPa, 60°C using 0.1 wt%, 0.5 wt% and 0.9 wt% MoDTC. To study the influence of contact pressure, tests were conducted with 0.5 wt% MoDTC at 400 rpm (0.6 m/s), 60°C. Tests were conducted at the following contact pressures; 0.98 GPa, 1.67 GPa, and 2.12 GPa. For repeatability, each test was carried out at least 2 times. There was good friction repeatability (3.2% error) calculated from the average friction values during the last one hour of the tests.

## **2.2 Wear analysis**

Optical images of wear scars generated on the tribopair after tests were obtained using an optical microscope. From these images, ball wear scar diameters (WSD) were determined. Wear from the discs has not been reported in this study since the widths of the wear scars were similar at different test conditions and the wear depths were too small to be detected by white light interferometry.

## **2.3 Chemical characterisation of wear scars**

Raman spectroscopy analysis was used to determine the chemical composition of the reaction products from the tribochemical reaction. After tests the tribopair samples were rinsed with heptane in an ultrasonic bath for 1 minute before Raman analysis. Although Raman analysis can be carried out on unrinsed samples, the samples in these tests were rinsed so as to obtain a good Raman signal of the MoDTC decomposition products. Unrinsed samples have a layer of lubricant on the surface and when analysed with Raman spectroscopy they show very strong peaks from the mineral base oil. The strong Raman peaks from the mineral base oil make it difficult for the rather weak peaks from MoDTC decomposition products to be observed.

Removing the lubricant from the sample by rinsing in heptane allowed Raman peaks from MoDTC decomposition products to be distinctly observed in the spectra.

Analysis of the wear scars was carried out with Renishaw Invia spectrometer (UK). Raman spectra were obtained with 488 nm wavelength laser at 1 mW laser power and 1s exposure time. Several accumulations were obtained in each spectrum so as to increase the signal-to-noise ratio. At these Raman acquisition parameters, determined in a previous study<sup>11</sup>, there is no laser damage to MoDTC tribofilms. All the Raman spectra were analysed using the Renishaw WiRE program for peak position.

### **3 Results**

#### **3.1 Influence of temperature**

Figure 1a shows friction coefficient values obtained during tests at different temperatures. For tests conducted at room temperature (20°C), friction was high ( $\mu=0.1$ ) at the beginning of the test and decreased gradually with rubbing time. The friction coefficient at the end of the test was 0.09. In tests carried out at 40°C, there was rapid friction drop to low steady friction values after an induction time of about 10 minutes. The friction coefficient after the friction drop was 0.07. Tests conducted at 60°C and 100°C also showed rapid friction drop to low values (0.05-0.06) after only a short induction time. It was noted that rapid friction drop was only observed when temperatures were increased from 20°C. Figure 1b shows the wear scar diameter (WSD) of wear scars formed on the balls at different temperatures. The WSD was highest at 20°C and decreased to lower values when the temperature was increased. In tests conducted with only the base oil, the WSD was 808  $\mu\text{m}$ . This was almost twice the WSD obtained when MoDTC lubricant was used. These results thus show that MoDTC reduced wear of the steel substrate in agreement with previous studies.<sup>12</sup>

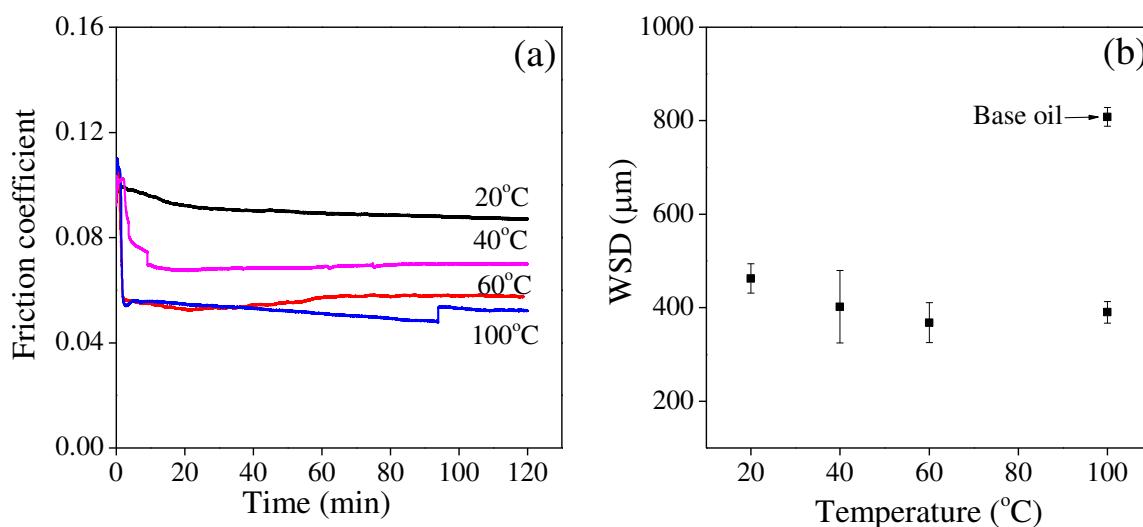


**Figure 1. (a) Friction coefficient obtained during tests (b) Ball wear scar diameters (WSD) after tests. Tests were conducted with 0.5 wt% MoDTC at 200 rpm, 2.12 GPa**

Figure 2 shows Raman spectra obtained from tribopair wear scars after tests at different temperatures. It should be highlighted that the chemical composition in the wear scars was non-uniform especially for tests conducted at 40°C and 60°C. Consequently, spectra obtained from different regions of the wear scars varied greatly. The spectra shown in Figure 2 only indicate the chemical composition at a given single spot within the wear scars.

Figure 2a shows a typical Raman spectrum obtained from the disc wear scar at 20°C. Spectra obtained from different regions on the tribopair wear scars are shown in Figure S1. In general, spectra obtained from different regions on the tribopair wear scars were very similar indicating spatial uniformity in chemical composition. The spectra had broad peaks at 335  $\text{cm}^{-1}$ , 453  $\text{cm}^{-1}$  and 925  $\text{cm}^{-1}$ . Spectra from the disc wear scar had an additional peak at 670  $\text{cm}^{-1}$  which was assigned to the formation of magnetite ( $\text{Fe}_3\text{O}_4$ ).<sup>13</sup>

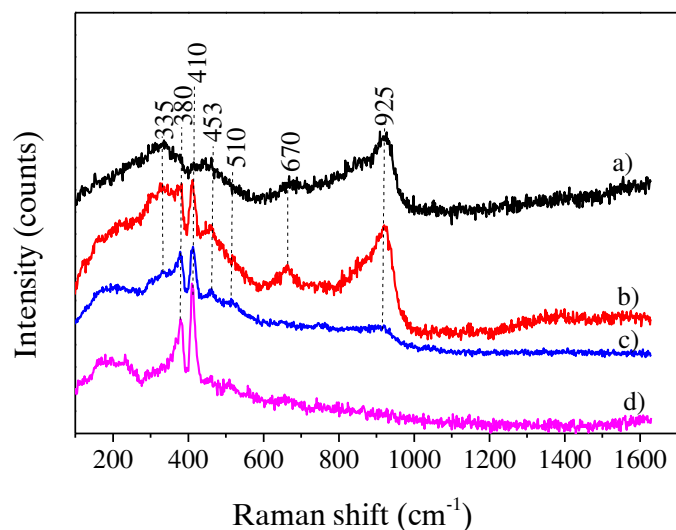


**Figure 2. Raman spectra obtained from tribopair wear scars after tests at different temperatures (a) 20°C (b) 40°C (c) 60°C (d) 100°C**

In previous Raman studies on the MoDTC additive, there have been no reports of spectra similar to those shown in Figure 2a. This can be due to the fact that no Raman analysis has been carried out on samples generated at 20°C. Most of the previous studies analysed samples generated at higher temperatures and Raman spectra showed MoS<sub>2</sub> peaks at 380 cm<sup>-1</sup> and 412 cm<sup>-1</sup>.<sup>5</sup> As will be shown later in this study, samples generated at higher temperatures do indeed have MoS<sub>2</sub> peaks but this was not the case for samples generated at lower temperatures. To the knowledge of the authors, this is the first time Raman peaks at 335 cm<sup>-1</sup>, 453 cm<sup>-1</sup> and 925 cm<sup>-1</sup> have been observed in tests with MoDTC. Observation of these peaks has given a new insight on the mechanism of MoDTC decomposition which is discussed in detail in Section 4.3.

It is possible that MoDTC decomposition did not occur at 20°C and that the chemical composition of the wear scars was due tests being conducted in base oil. In a previous study by the authors it was observed that in tribotests carried out in base oil the tribopair wear scars

were composed of hematite ( $\text{Fe}_2\text{O}_3$ ) and magnetite ( $\text{Fe}_3\text{O}_4$ ).<sup>11</sup> In Figure 2a, Raman peaks belonging to  $\text{Fe}_2\text{O}_3$  were not observed; only the peak at  $670\text{ cm}^{-1}$  belonging to  $\text{Fe}_3\text{O}_4$  was observed. Hence, the spectra observed in Figure 2a cannot be attributed to tests being conducted in mineral oil or from the mineral oil itself (Figure S10). The possibility that the spectra observed in Figure 2a were due to adsorbed MoDTC on the substrate was considered and Raman spectrum of MoDTC was investigated. Figure S10 shows the Raman spectrum obtained from the MoDTC additive concentrate. The spectrum of the additive has strong sharp peaks at  $971\text{ cm}^{-1}$  and  $430\text{ cm}^{-1}$  due to vibration of terminal oxygen atoms  $\nu(\text{Mo}=\text{O})$  and bridging sulphur atoms  $\nu(\text{Mo}-\text{S}_2-\text{Mo})$ , respectively.<sup>14, 15</sup> Peaks belonging to MoDTC additive were not observed in Figure 2a, indicating that adsorbed MoDTC was not present on the rubbing surfaces. It was therefore concluded that the broad peaks observed at  $335\text{ cm}^{-1}$ ,  $453\text{ cm}^{-1}$  and  $925\text{ cm}^{-1}$  in Figure 2a were due to chemical species formed as a result of MoDTC decomposition at the tribocontact.

From previous reports, probable MoDTC decomposition products are  $\text{MoO}_2$ <sup>16, 17</sup>,  $\text{MoO}_3$ <sup>10, 16</sup>,  $\text{MoS}_x\text{O}_{2-x}$ <sup>10</sup> and  $\text{MoS}_2$ <sup>18</sup>. These chemical species were previously identified using XPS. However, by carefully examining Raman spectra obtained from pure powders of  $\text{MoS}_2$ ,  $\text{MoO}_2$  and  $\text{MoO}_3$  (Figure S11) and those reported in literature<sup>19-24</sup>, it was concluded that  $\text{MoS}_2$ ,  $\text{MoO}_2$ ,  $\text{MoO}_3$  and  $\text{MoS}_x\text{O}_{2-x}$  were not present in MoDTC tribofilms generated at  $20^\circ\text{C}$ .

Based on reports in literature, the broad peak at  $925\text{ cm}^{-1}$  was assigned to  $\text{Mo}=\text{O}$  stretching in  $\text{FeMoO}_4$ .<sup>25-27</sup> This is the first time  $\text{FeMoO}_4$  is being reported as a product of MoDTC decomposition. Also from reports in literature, the broad peaks at  $335\text{ cm}^{-1}$  and  $453\text{ cm}^{-1}$  were assigned to the formation of amorphous sulphur-rich molybdenum compounds,  $\text{MoS}_x$  ( $x>2$ ), with bridging sulphur atoms ( $\text{S}_2^{2-}$ ).<sup>28-33</sup> Formation of amorphous  $\text{MoS}_x$  from MoDTC decomposition has not been reported in literature but examples of  $\text{MoS}_x$  compounds from decomposition of other compounds has been reported.<sup>31, 34-39</sup>

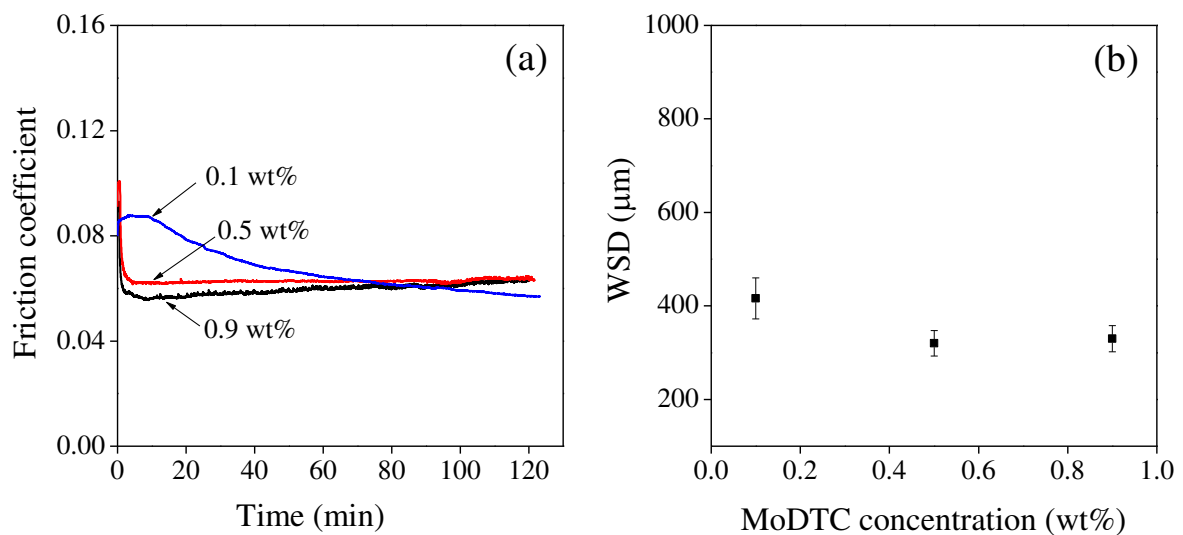
Figure 2b shows a typical spectrum obtained from the disc wear scar after tests at 40°C. Spectra obtained from different regions on the tribopair wear scars varied greatly as can be seen in Figure S2. Spectra obtained from some regions had broad peaks at 335 cm<sup>-1</sup>, 453 cm<sup>-1</sup> and 925 cm<sup>-1</sup>. In some regions, the MoS<sub>2</sub> A<sub>1g</sub> peak at 410 cm<sup>-1</sup> was observed emerging from the broad peak at 453 cm<sup>-1</sup>. In other regions, distinct MoS<sub>2</sub> peaks were observed at 381 cm<sup>-1</sup> (E<sup>1</sup><sub>2g</sub> peak) and 414 cm<sup>-1</sup> (A<sub>1g</sub> peak). The broad peak at 335 cm<sup>-1</sup> which became less intense when the E<sup>1</sup><sub>2g</sub> peak became distinct was attributed to ν(Mo-S) vibration in a structure containing bridging S<sub>2</sub><sup>2-</sup> ligands.<sup>31</sup> The broad peak at 453 cm<sup>-1</sup> disappeared when the MoS<sub>2</sub> A<sub>1g</sub> peak became distinct and less intense peaks were observed at 453 cm<sup>-1</sup> and 510 cm<sup>-1</sup>. The peak at 453 cm<sup>-1</sup> was assigned to ν(Mo-S) vibration while the peak at 510 cm<sup>-1</sup> was assigned to ν(S-S) vibration of terminal S<sub>2</sub><sup>2-</sup> ligands.<sup>31</sup> Overall, spectra obtained at 40°C indicated the presence of a mixture of Fe<sub>3</sub>O<sub>4</sub>, FeMoO<sub>4</sub>, MoS<sub>2</sub> and MoS<sub>x</sub>.

Figure 2c shows a typical Raman spectrum obtained from the disc wear scar after tests at 60°C. Spectra obtained from different regions of the tribopair wear scars are shown in Figure S3. Spectra from the ball wear scar were all very similar to each other and showed MoS<sub>2</sub> peaks. Spectra from the disc wear scar also showed MoS<sub>2</sub> peaks. In addition, peaks were also observed at 670 cm<sup>-1</sup> (Fe<sub>3</sub>O<sub>4</sub>) and 925 cm<sup>-1</sup> (FeMoO<sub>4</sub>). Overall, wear scars generated at 40°C were observed to have high amounts of MoS<sub>2</sub> and traces amounts of Fe<sub>3</sub>O<sub>4</sub> and FeMoO<sub>4</sub>.

Figure 2d shows a typical Raman spectrum obtained from the disc wear scar after tests at 100°C. The spectrum shows the presence of MoS<sub>2</sub> peaks. Spectra obtained from different regions on the tribopair wear scars (Figure S4) were similar to the spectrum in Figure 2d indicating uniformity in the chemical composition of the wear scars. The broad peak in the 100-250 cm<sup>-1</sup> region was attributed to stress-induced disorder in MoS<sub>2</sub> crystal structure.<sup>11, 40</sup>

### 3.2 Influence of MoDTC concentration

Figure 3a shows friction curves during tests at different MoDTC concentrations. The friction coefficient was high (0.10) at the beginning of the test in all tests. In the tests with 0.1 wt% MoDTC, the friction decreased gradually and reached 0.06 at the end of the test. In tests conducted with 0.5 wt% and 0.9 wt% MoDTC, high friction was only observed at the beginning of the test and rapidly dropped to low values (0.06) after a very short induction time. From wear results presented in Figure 3b it was observed that the WSD decreased slightly when MoDTC concentration was increased from 0.1 to 0.5 wt% and then remained low at higher concentrations.

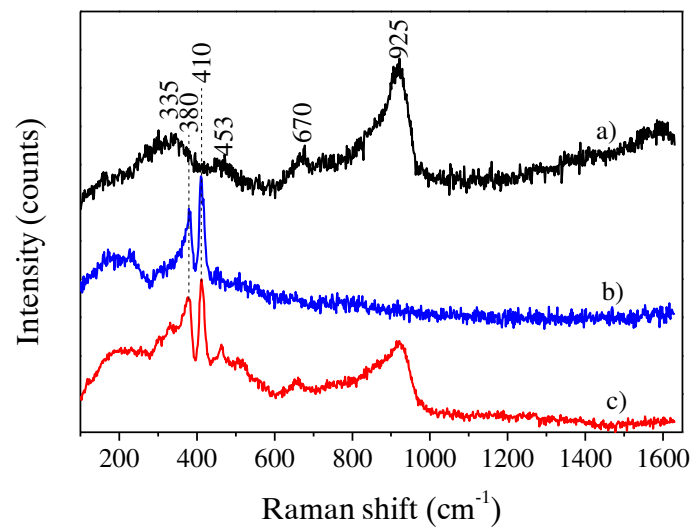


**Figure 3. (a) Friction curves during tests (b) Ball wear scar diameters (WSD) after tests.**

**Tests were conducted at varying MoDTC concentration at 60°C, 400 rpm, 1.67 GPa**

Figure 4 shows examples of typical spectra obtained from disc wear scars after tests at varying MoDTC concentrations. Figure 4a shows an example of a Raman spectrum obtained from the disc wear scar after tests using 0.1 wt% MoDTC. The spectrum indicates the presence of  $\text{Fe}_3\text{O}_4$ ,  $\text{FeMoO}_4$  and  $\text{MoS}_x$  within the wear scars. Spectra obtained from different regions of the tribopair wear scars showed a uniform chemical composition (Figure S5). Figure 4b shows a

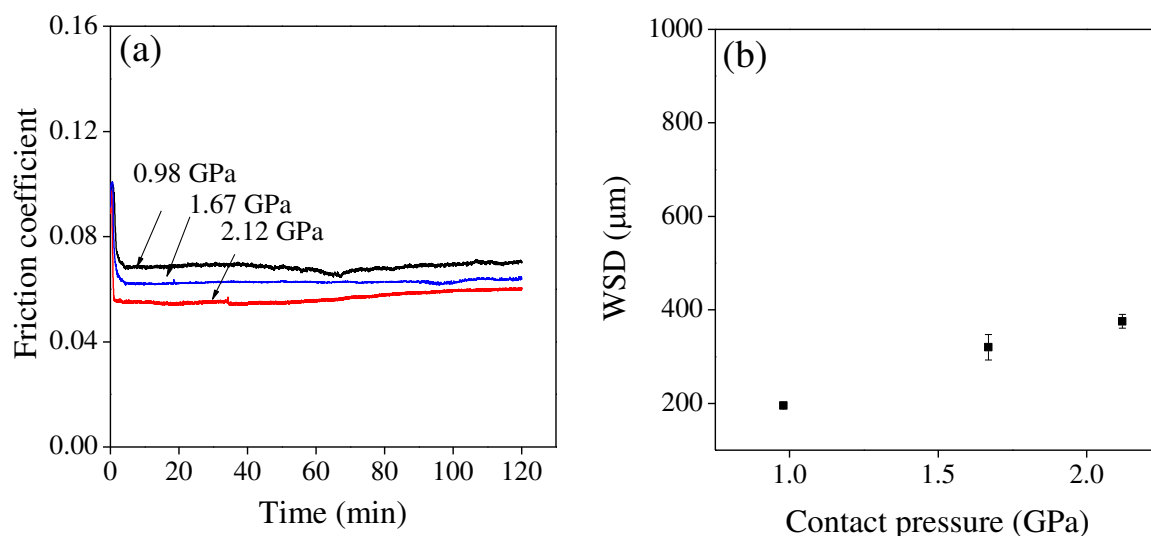
typical Raman spectrum obtained from the disc wear scar after tests with 0.5 wt% MoDTC. Spectra obtained from different regions of the tribopair wear scars (Figure S6) indicate the presence of MoS<sub>2</sub> with traces of FeMoO<sub>4</sub> and Fe<sub>3</sub>O<sub>4</sub>. Figure 4c shows a typical Raman spectrum obtained from the disc wear scar after tests using 0.9 wt% MoDTC. Spectra obtained from different regions on the tribopair wear scars varied from region to region as shown in Figure S7. In some regions, MoS<sub>2</sub> peaks were observed while in other regions peaks attributed from MoS<sub>x</sub>, Fe<sub>3</sub>O<sub>4</sub>, and FeMoO<sub>4</sub> were observed.



**Figure 4. Raman spectra obtained from the disc wear scars after tests at varying MoDTC concentrations (a) 0.1 wt% (b) 0.5 wt% (c) 0.9 wt%**

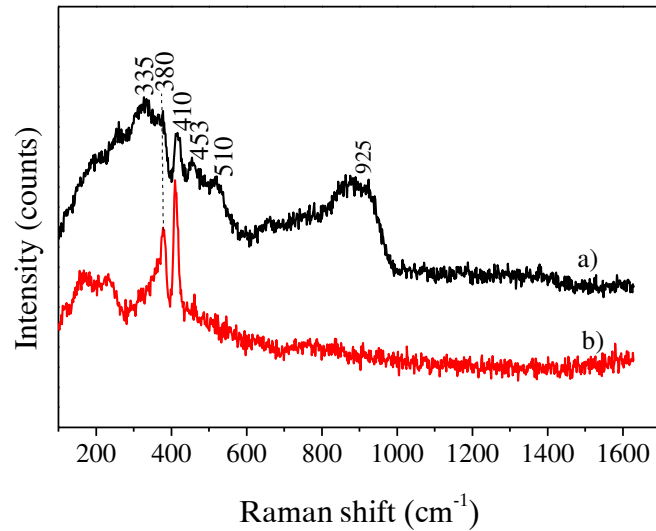
### 3.3 Influence of contact pressure

Figure 5a shows friction curves observed when tests were conducted at various contact pressures. The friction behaviour was similar at all pressures. There was high friction ( $\mu=0.10$ ) at the beginning of the test followed by rapid drop to low steady friction values ( $\mu=0.07-0.06$ ) after very short induction time. The WSD increased with increase in contact pressure as expected (Figure 5b).



**Figure 5. (a) Friction curves during tests (b) Ball wear scar diameters (WSD) after tests. Tests were conducted at varying contact pressures at 0.5 wt% MoDTC, 60°C, 400 rpm.**

Figure 6 shows representative Raman spectra obtained from tribopair wear scars after tests at 0.98 GPa and 2.12 GPa. Spectra obtained from different regions within the tribopair wear scars after tests at 0.98 GPa varied from spot to spot, especially on the ball wear scar (Figure S8). The Raman spectrum in Figure 6a shows that the wear scar was composed of a mixture of  $\text{MoS}_2$ ,  $\text{MoS}_x$  and  $\text{FeMoO}_4$ . A typical Raman spectrum obtained from tribopair wear scars after tests at 1.67 GPa was shown in Figure 4b. Figure 6b shows a typical Raman spectrum obtained from tribopair wear scars after tests at 2.12 GPa. The spectrum indicates that the wear scar was composed of  $\text{MoS}_2$ . Spectra obtained from different regions of the tribopair wear scar showed the chemical composition was uniform (Figure S9).



**Figure 6. Raman spectra obtained from the tribopair wear scar after tests at (a) 0.98 GPa (b) 2.12 GPa**

## 4 Discussion

### 4.1 MoS<sub>x</sub> and FeMoO<sub>4</sub> species

Tribological tests with MoDTC resulted in the formation of MoDTC tribofilms composed of MoS<sub>2</sub>, MoS<sub>x</sub> and FeMoO<sub>4</sub>. Although the formation of MoS<sub>2</sub> has been widely reported, the formation of FeMoO<sub>4</sub> and MoS<sub>x</sub> has not been reported before. Key information about these two compounds is presented below.

MoS<sub>x</sub> (x>2) compounds are normally formed at lower temperatures than MoS<sub>2</sub> and have been reported to undergo recrystallization at high temperatures to form MoS<sub>2</sub>.<sup>31, 39, 41-43</sup> Recrystallization of MoS<sub>x</sub> has also been observed under tribological conditions. Lince *et al.*<sup>44</sup> reported the formation of MoS<sub>2</sub> after tribological tests on MoS<sub>3</sub> coatings. Based on this information, it can be concluded that (1) MoS<sub>x</sub> is an intermediate compound in the formation of MoS<sub>2</sub> and (2) the transformation of MoS<sub>x</sub> to MoS<sub>2</sub> is dependent on temperature and shear stress.

Singer<sup>45</sup> reported that the formation of molybdenum oxides such as  $\text{Fe}_2\text{MoO}_4$  and  $\text{FeMoO}_4$  was possible in a system comprising of Fe, Mo, S and O. The formation of  $\text{FeMoO}_4$  has been reported when  $\text{MoS}_2$  coatings were rubbed with steel counterparts.<sup>46</sup> In literature, it has been reported that  $\text{Fe}_2(\text{MoO}_4)_3$  can be formed from a reaction of molybdenum compounds with  $\text{Fe}_2\text{O}_3$  at temperatures of about  $120^\circ\text{C}$ .<sup>47</sup> It has also been reported that metal molybdates can be formed at room temperature when mechanically activated (mechanical milling).<sup>48</sup> It is therefore not surprising that  $\text{FeMoO}_4$  was formed in tests with MoDTC lubricant since Fe, O and Mo were present at the contact. The formation of  $\text{FeMoO}_4$  in a system comprising of Fe, Mo and O was also confirmed by the authors by heating MoDTC at  $100^\circ\text{C}$  in the presence of  $\text{Fe}_3\text{O}_4$  (Figure S13). From reports in literature and results obtained in this study it can be deduced that in tribotests with MoDTC lubricant,  $\text{FeMoO}_4$  was probably formed from a reaction of molybdenum compounds with iron oxides on the steel surface. Also, that the reaction leading to the formation of  $\text{FeMoO}_4$  was mechanically-activated.

Previous XPS analysis of MoDTC tribofilms showed Mo 3d peaks at 229, 232.3 and 235 eV.<sup>10, 18</sup> From these XPS studies it was concluded that MoDTC tribofilms were composed of  $\text{MoO}_3$  due to the presence of Mo 3d<sub>5/2</sub> peak at 232.3 eV. The Mo 3d<sub>5/2</sub> peak for  $\text{FeMoO}_4$  is at 232.3 eV.<sup>26, 49</sup> Molybdenum in  $\text{MoO}_3$  and  $\text{FeMoO}_4$  have the same oxidation state (+6) therefore from XPS analysis it is impossible to differentiate the two compounds due to overlapping peaks. Raman spectra of  $\text{MoO}_3$ <sup>50</sup> and  $\text{FeMoO}_4$ <sup>25</sup> are completely different and can thus be used to distinguish the two compounds. In this study, Raman peaks belonging to  $\text{FeMoO}_4$  were observed while those belonging to  $\text{MoO}_3$  were not observed at all. It is possible that the Mo (6+) peak observed in MoDTC tribofilms using XPS analysis is probably due to the presence of  $\text{FeMoO}_4$  and not  $\text{MoO}_3$ .

## 4.2 Tribochemical reactions

In tests conducted at 20°C, it was observed that MoDTC decomposed to form MoS<sub>x</sub> and FeMoO<sub>4</sub> (Figure 2a). This is an interesting observation as such a reaction would not happen in non-tribological conditions since the temperature is too low to cause thermal decomposition of MoDTC. These results indicate that the tribochemical reaction was not only driven by temperature as is the case for thermally-activated reactions. The presence of shear stress in tribological tests also promoted the decomposition of MoDTC. This conclusion is supported by simulation studies conducted by Onodera *et al.*<sup>51</sup> where it was reported that decomposition of adsorbed MoDTC occurred only when pressure and sliding were applied. Numerical studies have shown that tribochemical reactions also occur in other molecules when shear stress is applied.<sup>52</sup> It is therefore suggested that the tribochemical reaction of MoDTC is best defined by Eq.1.<sup>53</sup>

$$k_{tribo} = A_o \exp \frac{\sigma V - E_a}{k_B T} \quad \text{Eq.1}$$

Where  $k_{tribo}$  is the reaction rate constant,  $A_o$  the pre-exponential factor,  $\sigma$  the shear stress,  $V$  the material constant,  $E_a$  the activation energy,  $T$  the temperature and  $k_B$  the Boltzmann constant. The shear stress component in Eq.1 provides additional energy which enables MoDTC decomposition to occur at low temperatures. The rate of MoDTC decomposition in tribological contacts is therefore dependent on shear stress, temperature as well as MoDTC concentration (Eq.2).

## 4.3 Newly proposed decomposition mechanism

The mechanism for MoDTC decomposition proposed by Grossiord *et al.*<sup>10</sup> cannot be used to explain MoDTC decomposition products obtained in 20°C tests since MoS<sub>2</sub>, MoO<sub>2</sub> or MoO<sub>3</sub> were not detected in the wear scars. The previously proposed mechanism suggests the

formation of MoO<sub>2</sub> and MoO<sub>3</sub> however these oxides were not detected by Raman spectroscopy in this study. There is therefore a need to propose a decomposition pathway for MoDTC that would accommodate the observations made in this study.

In determining the new reaction pathway, the chemical composition of MoDTC tribofilms formed at various contact parameters was considered. As discussed in Section 4.2, shear stress participates in the decomposition of MoDTC probably through rupturing of bonds. To determine which bonds would be most susceptible to rupturing under shear stress, bond dissociation energies of bonds in MoDTC were obtained from literature. From bond dissociation energies for various bonds in MoDTC (Table S1), the C-S bond has the lowest bond dissociation energy therefore it is the weakest bond and can be easily ruptured under shear stress.<sup>53,54</sup> Cleavage of C-S bond in dithiocarbamates has been proposed in literature.<sup>55</sup> Figure 7 shows the proposed reaction pathway for MoDTC decomposition initiated by shear stress.

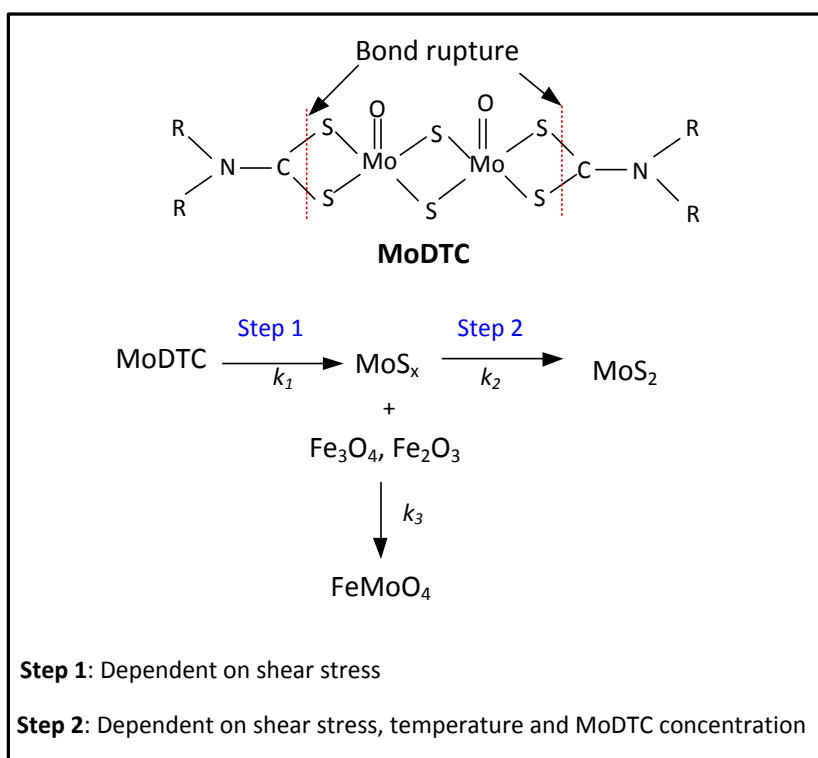


**Figure 7. Proposed reaction pathway for decomposition of MoDTC within tribocontacts**

The decomposition process occurs as follows.

- MoDTC first adsorbs on the tribopair surfaces.<sup>51</sup>
- In Step 1, shear stress applied on adsorbed MoDTC molecules causes decomposition to occur. The decomposition process begins by rupturing of C-S bonds forming molybdenum intermediate compound which undergoes intramolecular sulphonation forming amorphous MoS<sub>x</sub>.
- In Step 2, MoS<sub>x</sub> is converted to MoS<sub>2</sub>. Since MoS<sub>x</sub> is formed at lower temperatures than MoS<sub>2</sub>, the activation energy for formation of MoS<sub>x</sub> is lower than that for the formation of MoS<sub>2</sub>. Therefore, MoS<sub>2</sub> can be formed from MoS<sub>x</sub> either through increasing the energy at the contact by increasing temperature or increasing shear stress.
- FeMoO<sub>4</sub> is formed from a reaction of iron oxides on the steel surfaces with MoS<sub>x</sub>.

The rates of reactions for formation of the various molybdenum species are shown in Eq 2-4. It should be noted that these are simplified expressions as the order of the reactions is currently unknown.

$$r_{MoS_x} = k_1[MoDTC] \quad \text{Eq.2}$$

$$r_{MoS_2} = k_2[MoS_x] \quad \text{Eq.3}$$

$$r_{FeMoO_4} = k_3[MoS_x] [iron\ oxides] \quad \text{Eq.4}$$

Although the exact values for reaction rate constants  $k_1$ ,  $k_2$  and  $k_3$  has not been determined in this study, it is believed that the reaction constants can be described by Eq.1.

Reaction constant  $k_1$  is not dependent on temperature as MoS<sub>x</sub> is formed even at 20°C given that shear stress is applied. Reaction constant  $k_2$  is dependent on both temperature and shear stress since recrystallization of MoS<sub>x</sub> is dependent on these two parameters (Section 4.1). Varying the temperature and shear stress will therefore affect  $k_2$  values which will in turn affect the molybdenum sulphide compound formed as follows.

$k_1 \gg k_2$	MoS <sub>x</sub>
$k_1 > k_2$	MoS <sub>x</sub> , MoS <sub>2</sub>
$k_1 \ll k_2$	MoS <sub>2</sub>

In Figure 2, it was also shown that the amount of MoS<sub>2</sub> increased while the amount of FeMoO<sub>4</sub> decreased with increase in temperature. This observation suggests that two competing reactions occur at the tribocontact; (1) oxidation of the surface and (2) formation of MoS<sub>2</sub>. Formation of FeMoO<sub>4</sub> is dependent on the presence of iron oxides at the tribocontact. Iron oxides are formed as a result of surface oxidation. Oxidation of the steel substrate is favoured when the formation of MoS<sub>2</sub> at the contact is inhibited. On the other hand, rapid formation of MoS<sub>2</sub> at the contact will hinder surface oxidation and the subsequent formation of FeMoO<sub>4</sub>.

#### 4.4 Effect of temperature and MoDTC concentration

Results presented in Figure 2 showed that the chemical composition of MoDTC tribofilms changed from MoS<sub>x</sub>, FeMoO<sub>4</sub> to MoS<sub>2</sub> when the temperature was increased from 20°C to 100°C. These observations have not been reported elsewhere in literature. In the study by Morina *et al.*<sup>7</sup> it was reported that MoDTC tribofilms formed at 30°C had lower amounts of Mo and S than those formed at higher temperatures (100-150°C). It was also reported in the same study that more Mo oxides (MoO<sub>3</sub>) were formed at 30°C than at higher temperatures.

MoDTC concentration was also found to affect the composition of MoDTC tribofilms in this study (Figure 4). At a low concentration of 0.1 wt%, MoS<sub>x</sub> and FeMoO<sub>4</sub> were formed while at 0.5 wt%, MoS<sub>2</sub> was formed. MoDTC tribofilms formed at 0.9 wt% were comprised of a mixture of MoS<sub>2</sub>, MoS<sub>x</sub> and FeMoO<sub>4</sub>. In a previous study, it was reported that sulphates were formed at low MoDTC concentrations (Mo 100 ppm) while MoS<sub>2</sub> was formed at high concentrations.<sup>9</sup> In another study, it was reported that the amount of MoS<sub>2</sub> increased with MoDTC concentration.<sup>56</sup>

Reports in literature on the influence of temperature and MoDTC concentration on the composition of MoDTC tribofilms are not in complete agreement with findings in this study. This can be due to differences in analysis techniques used in this study and in the previous studies. This is because different techniques have varying capabilities when distinguishing molybdenum compounds.

Temperature and MoDTC concentration affect MoDTC decomposition in the following three ways. (1) Affecting the adsorption of MoDTC on rubbing surfaces (2) determining the nature of products formed (3) affecting the rate of the MoDTC decomposition. Adsorption of additives has been shown to increase with increase in temperature and concentration.<sup>57, 58</sup> At low MoDTC concentrations and low temperatures, there is less MoDTC adsorbed on the surface. Lower MoDTC coverage will promote oxidation of the steel surface while higher MoDTC coverage will hinder oxidation of the steel surface. From the discussion presented in Section 4.3, it can be seen that high temperatures will promote the formation of MoS<sub>2</sub> formed while low temperatures will lead to formation of MoS<sub>x</sub>. High temperatures will also lead to rapid formation of MoS<sub>2</sub> (Eq.1). Also, from Eq.2, it can be seen that high MoDTC concentrations will increase the rate of MoS<sub>x</sub> formation. These insights on MoDTC adsorption and decomposition can be used to explain the trends observed in this study at varying temperatures and MoDTC concentrations.

Observations made at varying temperatures can be explained as follows. The formation of FeMoO<sub>4</sub> at low temperatures is due high surface oxidation due to low MoDTC coverage. The decrease in FeMoO<sub>4</sub> amount with increase in temperature is due to a decrease in surface oxidation as formation of MoS<sub>2</sub> on the surface occurs.

Observations made at varying MoDTC concentrations can be explained as follows. At low concentrations, FeMoO<sub>4</sub> is formed due to the presence of an oxidised surface as a result of low

MoDTC coverage. At the temperature used (60°C), the formation of MoS<sub>2</sub> was expected. However, MoS<sub>x</sub> was formed instead of MoS<sub>2</sub>. The formation of MoS<sub>x</sub> can be attributed to the slow rate of MoS<sub>x</sub> formation due to a lower MoDTC concentration (Eq.2). Consequently, the rate of MoS<sub>x</sub> conversion to MoS<sub>2</sub> would be very slow because of low MoS<sub>x</sub> concentration (Eq.3). The formation of MoS<sub>2</sub> would therefore require a longer time than the duration used in the test (2h). Increasing MoDTC concentration from 0.1 wt% to 0.5 wt% resulted in the formation of MoS<sub>2</sub> as expected. This could be because the formation of MoS<sub>x</sub> was faster. Increasing the concentration further to 0.9 wt% MoDTC resulted in a mixture of MoS<sub>x</sub> and MoS<sub>2</sub> which was unexpected. This observation can be due to the rate of MoS<sub>x</sub> formation being too high to balance the rate of MoS<sub>2</sub> formation. To increase the rate of MoS<sub>2</sub> formation,  $k_2$  values have to be increased. This can be done either by increasing the temperature or the shear stress.

#### **4.5 Relationship between friction and chemical composition of MoDTC tribofilms**

As it is well known, friction reduction by MoDTC is due to the formation of tribofilms composed of MoS<sub>2</sub>. However, this study has shown that in certain test conditions MoS<sub>x</sub> and FeMoO<sub>4</sub> can be formed and this affects the friction behaviour. In test conditions where MoS<sub>2</sub> was formed, there was a rapid drop in friction to low values after a short induction time. The mechanism by which MoS<sub>2</sub> reduces friction was reported by Onodera *et al.*<sup>59</sup> When MoS<sub>x</sub> and FeMoO<sub>4</sub> were formed, the friction reduction was gradual. Friction reduction was achieved due to the presence of MoS<sub>x</sub> as FeMoO<sub>4</sub> does not have any friction reducing capabilities.<sup>44</sup> Friction reduction with MoS<sub>x</sub> is however less compared to that achieved with MoS<sub>2</sub>. In tests where MoS<sub>x</sub>, MoS<sub>2</sub> and FeMoO<sub>4</sub> were observed at the tribocontact, the friction values were slightly lower than those observed when only MoS<sub>x</sub> and FeMoO<sub>4</sub> were present at the tribocontact. These results indicate that the chemical composition of MoDTC tribofilms determines the friction observed. Thus the intermediate friction values observed in previous studies<sup>4,5</sup> can be

explained by the presence of  $\text{MoS}_2$ ,  $\text{MoS}_x$  and  $\text{FeMoO}_4$  at the tribocontact in varying proportions.

#### **4.6 Effect of contact parameters on wear**

It was observed that the ball WSD decreased by about 50% when MoDTC was added to BO. This is in agreement with previous studies.<sup>12, 56</sup> Wear reduction can be attributed to the formation of MoDTC tribofilms. It has been reported that MoDTC tribofilms have a lower hardness (0.4-0.5 GPa) than steel.<sup>60</sup> This means that, the tribofilms can be easily sheared instead of the steel substrate. This way MoDTC tribofilms protect the substrate from wear.

Larger WSD were observed at low temperatures (20°C) and low concentrations (0.1 wt%). At these conditions, it was also observed that the induction time was longer than that observed at higher temperatures and higher concentrations. The longer induction times indicate that the formation of MoDTC tribofilms was delayed. The absence of MoDTC tribofilms during the long induction period could explain the slightly higher wear observed at low temperatures and low MoDTC concentrations.

### **5 Conclusions**

This study has investigated the influence of temperature, MoDTC concentration and contact pressure on the MoDTC decomposition within tribological contacts. Chemical composition of wear scars after tribological tests was conducted using Raman spectroscopy. Results show that MoDTC decomposition in steel/steel contacts is highly dependent on test conditions. MoDTC decomposes to form  $\text{MoS}_2$ ,  $\text{FeMoO}_4$  and  $\text{MoS}_x$  depending on tests conditions. The various MoDTC decomposition products formed within the tribocontact determine the friction performance. Low friction was observed when  $\text{MoS}_2$  was formed while high friction values were obtained when  $\text{MoS}_x$  and  $\text{FeMoO}_4$  were formed.  $\text{MoS}_x$  formed at low temperatures was converted to  $\text{MoS}_2$  at higher temperatures indicating that  $\text{MoS}_x$  was an intermediate compound

in the formation of MoS<sub>2</sub>. Furthermore, it has been shown that ferrous surfaces participate in the decomposition of MoDTC by reacting with the decomposition products to form FeMoO<sub>4</sub>. Based on Raman analysis results obtained in this study, a new decomposition pathway for MoDTC in tribological contacts has been proposed.

## Acknowledgement

This study was funded by the FP7 program through the Marie Curie Initial Training Network (MC-ITN) entitled “ENTICE - Engineering Tribochemistry and Interfaces with a Focus on the Internal Combustion Engine” [290077] and was carried out at University of Leeds, UK.

## References

1. Farmer, H. H.; Rowan, E. V., Molybdenum oxysulfide dithiocarbamates and processes for their preparation. Google Patents: 1967.
2. Sanin, P. I.; Kuz'mina, G. N.; Lozovoi, Y. A.; Zaimovskaya, T. A., Molybdenum complexes as synthetic additives to lubricating oils. *Petroleum Chemistry U.S.S.R.* **1986**, *26* (4), 252-257.
3. Yamamoto, Y.; Gondo, S., Friction and Wear Characteristics of Molybdenum Dithiocarbamate and Molybdenum Dithiophosphate. *Tribology Transactions* **1989**, *32* (2), 251-257.
4. Graham, J.; Spikes, H.; Korcek, S., The friction reducing properties of molybdenum dialkyldithiocarbamate additives: Part I - Factors influencing friction reduction. *Tribology Transactions* **2001**, *44* (4), 626-636.
5. Miklozic, K. T.; Graham, J.; Spikes, H., Chemical and physical analysis of reaction films formed by molybdenum dialkyl-dithiocarbamate friction modifier additive using Raman and atomic force microscopy. *Tribology Letters* **2001**, *11* (2), 71-81.
6. Graham, J.; Spikes, H.; Jensen, R., The friction reducing properties of molybdenum dialkyldithiocarbamate additives: Part II - Durability of friction reducing capability. *Tribology Transactions* **2001**, *44* (4), 637-647.
7. Morina, A.; Neville, A.; Priest, M.; Green, J. H., ZDDP and MoDTC interactions in boundary lubrication—The effect of temperature and ZDDP/MoDTC ratio. *Tribology International* **2006**, *39* (12), 1545-1557.
8. Sakurai, T.; Okabe, H.; Isoyama, H., The Synthesis of Di- $\mu$ -thio-dithio-bis (dialkyldithiocarbamates) Dimolybdenum (V) and Their Effects on Boundary Lubrication. *Bulletin of The Japan Petroleum Institute* **1971**, *13* (2), 243-249.
9. Kasrai, M.; Cutler, J. N.; Gore, K.; Canning, G.; Bancroft, G. M.; Tan, K. H., The Chemistry of Antiwear Films Generated by the Combination of ZDDP and MoDTC Examined by X-ray Absorption Spectroscopy. *Tribology Transactions* **1998**, *41* (1), 69-77.
10. Grossiord, C.; Varlot, K.; Martin, J. M.; Le Mogne, T.; Esnouf, C.; Inoue, K., MoS<sub>2</sub> single sheet lubrication by molybdenum dithiocarbamate. *Tribology International* **1998**, *31* (12), 737-743.

11. Khaemba, D.; Neville, A.; Morina, A., A methodology for Raman characterisation of MoDTC tribofilms and its application in investigating the influence of surface chemistry on friction performance of MoDTC lubricants. *Tribology Letters* **2015**, *59* (3), 1-17.
12. Vengudusamy, B.; Green, J. H.; Lamb, G. D.; Spikes, H. A., Behaviour of MoDTC in DLC/DLC and DLC/steel contacts. *Tribology International* **2012**, *54*, 68-76.
13. Colombaro, P.; Cherifi, S.; Despert, G., Raman identification of corrosion products on automotive galvanized steel sheets. *Journal of Raman Spectroscopy* **2008**, *39* (7), 881-886.
14. Müller, A.; Bhattacharyya, R. G.; Mohan, N.; Pfeifferkorn, B., On the preparation of binuclear S, S bridged molybdenum(V) complexes crystal and molecular structure of [Mo<sub>2</sub>S<sub>4</sub>(Et<sub>2</sub>dtc)<sub>2</sub>]. *Zeitschrift für anorganische und allgemeine Chemie* **1979**, *454* (1), 118-124.
15. Ueyama, N.; Nakata, M.; Araki, T.; Nakamura, A.; Yamashita, S.; Yamashita, T., Raman and resonance Raman spectra of sulphur-bridged binuclear molybdenum (V) complexes of cysteine-containing chelate anions. *Chemistry Letters* **1979**, *8* (4), 421-424.
16. Morina, A.; Neville, A.; Priest, M.; Green, J. H., ZDDP and MoDTC interactions and their effect on tribological performance - Tribofilm characteristics and its evolution. *Tribology Letters* **2006**, *24* (3), 243-256.
17. Muraki, M.; Yanagi, Y.; Sakaguchi, K., Synergistic effect on frictional characteristics under rolling-sliding conditions due to a combination of molybdenum dialkyldithiocarbamate and zinc dialkyldithiophosphate. *Tribology International* **1997**, *30* (1), 69-75.
18. Unnikrishnan, R.; Jain, M. C.; Harinarayan, A. K.; Mehta, A. K., Additive-additive interaction: An XPS study of the effect of ZDDP on the AW/EP characteristic of molybdenum based additives. *Wear* **2002**, *252* (3-4), 240-249.
19. Spevack, P. A.; McIntyre, N. S., Thermal reduction of molybdenum trioxide. *The Journal of Physical Chemistry* **1992**, *96* (22), 9029-9035.
20. Can, L.; Zhengcao, L.; Zhengjun, Z., MoO<sub>x</sub> thin films deposited by magnetron sputtering as an anode for aqueous micro-supercapacitors. *Science and Technology of Advanced Materials* **2013**, *14* (6), 065005.
21. Lee, S.-H.; Seong, M. J.; Tracy, C. E.; Mascarenhas, A.; Pitts, J. R.; Deb, S. K., Raman spectroscopic studies of electrochromic α-MoO<sub>3</sub> thin films. *Solid State Ionics* **2002**, *147* (1-2), 129-133.
22. Schrader, G. L.; Cheng, C. P., In situ laser Raman spectroscopy of the sulfiding of Moγ-Al<sub>2</sub>O<sub>3</sub> catalysts. *Journal of Catalysis* **1983**, *80* (2), 369-385.
23. Wei, Z.; Xin, Q.; Xiong, G., Investigation of the sulfidation of Mo/TiO<sub>2</sub>-Al<sub>2</sub>O<sub>3</sub> catalysts by TPS and LRS. *Catal Lett* **1992**, *15* (3), 255-267.
24. Haro-Poniatowski, E.; Julien, C.; Pecquenard, B.; Livage, J.; Camacho-López, M. A., Laser-induced structural transformations in MoO<sub>3</sub> investigated by Raman spectroscopy. *Journal of Materials Research* **1998**, *13* (04), 1033-1037.
25. Wang, Y.; He, P.; Lei, W.; Dong, F.; Zhang, T., Novel FeMoO<sub>4</sub>/graphene composites based electrode materials for supercapacitors. *Composites Science and Technology* **2014**, *103* (0), 16-21.
26. Zhang, Z.; Li, W.; Ng, T.-W.; Kang, W.; Lee, C.-S.; Zhang, W., Iron(ii) molybdate (FeMoO<sub>4</sub>) nanorods as a high-performance anode for lithium ion batteries: structural and chemical evolution upon cycling. *Journal of Materials Chemistry A* **2015**, *3* (41), 20527-20534.
27. Kuang, W.; Fan, Y.; Chen, Y., State and Reactivity of Lattice Oxygen Ions in Mixed Fe-Mo Oxides. *Langmuir* **2000**, *16* (3), 1440-1443.

28. Müller, A.; Jostes, R.; Jaegermann, W.; Bhattacharyya, R., Spectroscopic investigation on the molecular and electronic structure of  $[\text{Mo}_3\text{S}_{13}]^{2-}$ , a discrete binary transition metal sulfur cluster. *Inorganica Chimica Acta* **1980**, *41* (0), 259-263.
29. Maezawa, A.; Kitamura, M.; Okamoto, Y.; Imanaka, T., Characterization of Active Sites in Sulfided Molybdenum/ Alumina Hydrodesulfurization Catalysts. *Bulletin of the Chemical Society of Japan* **1988**, *61* (7), 2295-2301.
30. Sekine, T.; Uchinokura, K.; Nakashizu, T.; Matsuura, E.; Yoshizaki, R., Dispersive Raman Mode of Layered Compound 2H-MoS<sub>2</sub> under the Resonant Condition. *Journal of the Physical Society of Japan* **1984**, *53* (2), 811-818.
31. Weber, T.; Muijsers, J. C.; Niemantsverdriet, J. W., Structure of Amorphous MoS<sub>3</sub>. *The Journal of Physical Chemistry* **1995**, *99* (22), 9194-9200.
32. Müller, A.; Nolte, W.-O.; Krebs, B.,  $[(\text{S}_2)_2\text{Mo}(\text{S}_2)_2\text{Mo}(\text{S}_2)_2]^{2-}$ , a Novel Complex Containing Only S<sup>2-</sup> Ligands and a Mo-Mo Bond. *Angewandte Chemie International Edition in English* **1978**, *17* (4), 279-279.
33. Müller, A.; Weinstock, N.; Schulze, H., Laser-Raman-Spektren der Ionen MoS<sub>4</sub><sup>2-</sup>, WS<sub>4</sub><sup>2-</sup>, MoOS<sub>3</sub><sup>2-</sup> und WOS<sub>3</sub><sup>2-</sup> in wässriger Lösung sowie der entsprechenden kristallinen Alkalisalze. *Spectrochimica Acta Part A: Molecular Spectroscopy* **1972**, *28* (6), 1075-1082.
34. Chang, C. H.; Chan, S. S., Infrared and Raman studies of amorphous MoS<sub>3</sub> and poorly crystalline MoS<sub>2</sub>. *Journal of Catalysis* **1981**, *72* (1), 139-148.
35. Wang, T.; Zhuo, J.; Du, K.; Chen, B.; Zhu, Z.; Shao, Y.; Li, M., Electrochemically Fabricated Polypyrrole and MoS<sub>x</sub> Copolymer Films as a Highly Active Hydrogen Evolution Electrocatalyst. *Advanced Materials* **2014**, *26* (22), 3761-3766.
36. Bhattacharya, R. N.; Lee, C. Y.; Pollak, F. H.; Schleich, D. M., Optical study of amorphous MoS<sub>3</sub>: Determination of the fundamental energy gap. *Journal of Non-Crystalline Solids* **1987**, *91* (2), 235-242.
37. Sourisseau, C.; Gorochoy, O.; Schleich, D. M., Comparative IR and Raman studies of various amorphous MoS<sub>3</sub> and Li<sub>x</sub>MoS<sub>3</sub> phases. *Materials Science and Engineering: B* **1989**, *3* (1-2), 113-117.
38. Khudorozhko, G. F.; Bulusheva, L. G.; Mazalov, L. N.; Fedorov, V. E.; Morales, J.; Kravtsova, E. A.; Asanov, I. P.; Parygina, G. K.; Mironov, Y. V., Synthesis and study of the electronic structure of molybdenum tetrasulfide and its lithium intercalates. *Journal of Physics and Chemistry of Solids* **1998**, *59* (2), 283-288.
39. Rice, D. A.; Hibble, S. J.; Almond, M. J.; Mohammad, K. A. H.; Pearse, S. P., Novel low-temperature route to known (MnS and FeS<sub>2</sub>) and new (CrS<sub>3</sub>, MoS<sub>4</sub> and WS<sub>5</sub>) transition-metal sulfides. *Journal of Materials Chemistry* **1992**, *2* (8), 895-896.
40. McDevitt, N. T.; Bultman, J. E.; Zabinski, J. S., Study of Amorphous MoS<sub>2</sub> Films Grown by Pulsed Laser Deposition. *Appl. Spectrosc.* **1998**, *52* (9), 1160-1164.
41. Weber, T.; Muijsers, J. C.; van Wolput, J. H. M. C.; Verhagen, C. P. J.; Niemantsverdriet, J. W., Basic Reaction Steps in the Sulfidation of Crystalline MoO<sub>3</sub> to MoS<sub>2</sub>, As Studied by X-ray Photoelectron and Infrared Emission Spectroscopy. *The Journal of Physical Chemistry* **1996**, *100* (33), 14144-14150.
42. Wildervanck, J. C.; Jellinek, F., Preparation and Crystallinity of Molybdenum and Tungsten Sulfides. *Zeitschrift für anorganische und allgemeine Chemie* **1964**, *328* (5-6), 309-318.
43. Li, X.; Zhang, W.; Wu, Y.; Min, C.; Fang, J., Solution-Processed MoS<sub>x</sub> as an Efficient Anode Buffer Layer in Organic Solar Cells. *ACS Applied Materials & Interfaces* **2013**, *5* (18), 8823-8827.

44. Lince, J.; Pluntze, A.; Jackson, S.; Radhakrishnan, G.; Adams, P., Tribochemistry of MoS<sub>3</sub> Nanoparticle Coatings. *Tribology Letters* **2014**, *53* (3), 543-554.
45. Singer, I., A thermochemical model for analyzing low wear-rate materials. *Surface and Coatings Technology* **1991**, *49* (1), 474-481.
46. Fayeulle, S.; Ehni, P. D.; Singer, I. L., Paper V (ii) Role of transfer films in wear of MoS<sub>2</sub> coatings. In *Tribology Series*, D. Dowson, C. M. T.; Godet, M., Eds. Elsevier: 1990; Vol. Volume 17, pp 129-138.
47. Bowker, M.; Brookes, C.; Carley, A. F.; House, M. P.; Kosif, M.; Sankar, G.; Wawata, I.; Wells, P. P.; Yaseneva, P., Evolution of active catalysts for the selective oxidative dehydrogenation of methanol on Fe<sub>2</sub>O<sub>3</sub> surface doped with Mo oxide. *Physical Chemistry Chemical Physics* **2013**, *15* (29), 12056-12067.
48. Temuujin, J.; MacKenzie, K. J. D.; Burmaa, G.; Tsend-Ayush, D.; Jadambaa, T.; Riessen, A. v., Mechanical activation of MoS<sub>2</sub> + Na<sub>2</sub>O<sub>2</sub> mixtures. *Minerals Engineering* **2009**, *22* (4), 415-418.
49. Zhang, Z.; Hu, C.; Hashim, M.; Chen, P.; Xiong, Y.; Zhang, C., Synthesis and magnetic property of FeMoO<sub>4</sub> nanorods. *Materials Science and Engineering: B* **2011**, *176* (9), 756-761.
50. Windom, B.; Sawyer, W. G.; Hahn, D., A Raman Spectroscopic Study of MoS<sub>2</sub> and MoO<sub>3</sub>: Applications to Tribological Systems. *Tribology Letters* **2011**, *42* (3), 301-310.
51. Onodera, T.; Miura, R.; Suzuki, A.; Tsuboi, H.; Hatakeyama, N.; Endou, A.; Takaba, H.; Kubo, M.; Miyamoto, A., Development of a quantum chemical molecular dynamics tribochemical simulator and its application to tribochemical reaction dynamics of lubricant additives. *Modelling and Simulation in Materials Science and Engineering* **2010**, *18* (3), 034009.
52. Haw, S. M.; Mosey, N. J., Tribochemistry of Aldehydes Sheared between (0001) Surfaces of  $\alpha$ -Alumina from First-Principles Molecular Dynamics. *The Journal of Physical Chemistry C* **2012**, *116* (3), 2132-2145.
53. Mahrova, M.; Conte, M.; Roman, E.; Nevshupa, R., Critical Insight into Mechanochemical and Thermal Degradation of Imidazolium-Based Ionic Liquids with Alkyl and Monomethoxypoly(ethylene glycol) Side Chains. *The Journal of Physical Chemistry C* **2014**, *118* (39), 22544-22552.
54. Adams, H. L.; Garvey, M. T.; Ramasamy, U. S.; Ye, Z.; Martini, A.; Tysoe, W. T., Shear-Induced Mechanochemistry: Pushing Molecules Around. *The Journal of Physical Chemistry C* **2015**, *119* (13), 7115-7123.
55. Coffey, T. A.; Forster, G. D.; Hogarth, G., Molybdenum(VI) imidodisulfur complexes formed via double sulfur-carbon bond cleavage of dithiocarbamates. *Journal of the Chemical Society, Dalton Transactions* **1996**, (2), 183-193.
56. Yamamoto, Y.; Gondo, S.; Kamakura, T.; Tanaka, N., Frictional characteristics of molybdenum dithiophosphates. *Wear* **1986**, *112* (1), 79-87.
57. Dacre, B.; Bovington, C. H., The Adsorption and Desorption of Zinc Diisopropylidithiophosphate on Steel. *A S L E Transactions* **1982**, *25* (4), 546-554.
58. Vengudusamy, B.; Grafl, A.; Novotny-Farkas, F.; Schöfmann, W., Influence of Surface Roughness on the Tribological Behavior of Gear Oils in Steel-Steel Contacts: Part I—Boundary Friction Properties. *Tribology Transactions* **2014**, *57* (2), 256-266.
59. Onodera, T.; Morita, Y.; Suzuki, A.; Koyama, M.; Tsuboi, H.; Hatakeyama, N.; Endou, A.; Takaba, H.; Kubo, M.; Dassenoy, F.; Minfray, C.; Joly-Pottuz, L.; Martin, J.-M.; Miyamoto, A., A Computational Chemistry Study on Friction of h-MoS<sub>2</sub>. Part I. Mechanism of Single Sheet Lubrication. *The Journal of Physical Chemistry B* **2009**, *113* (52), 16526-16536.

60. Bec, S.; Tonck, A.; Georges, J. M.; Roper, G. W., Synergistic Effects of MoDTC and ZDTP on Frictional Behaviour of Tribofilms at the Nanometer Scale. *Tribology Letters* **2004**, *17* (4), 797-809.